

In Vivo Measurement of Hindlimb Dorsiflexor Isometric Torque from Pig

Benjamin T. Corona¹, Jarrod A. Call^{2,3}, Matthew Borkowski⁴, Sarah M. Greising⁵

¹ School of Medicine, Wake Forest University ² Department of Kinesiology, University of Georgia ³ Regenerative Bioscience Center, University of Georgia ⁴ Aurora Scientific Inc. ⁵ School of Kinesiology, University of Minnesota

Corresponding Author

Sarah M. Greising

grei0064@umn.edu

Citation

Corona, B.T., Call, J.A., Borkowski, M., Greising, S.M. *In Vivo* Measurement of Hindlimb Dorsiflexor Isometric Torque from Pig. *J. Vis. Exp.* (175), e62905, doi:10.3791/62905 (2021).

Date Published

September 3, 2021

DOI

10.3791/62905

URL

jove.com/video/62905

Abstract

Reliable assessment of skeletal muscle strength is arguably the most important outcome measure in neuromuscular and musculoskeletal disease and injury studies, particularly when evaluating regenerative therapies' efficacy. Additionally, a critical aspect of translating many regenerative therapies is the demonstration of scalability and effectiveness in a large animal model. Various physiological preparations have been established to evaluate intrinsic muscle function properties in basic science studies, primarily in small animal models. The practices may be categorized as: *in vitro* (isolated fibers, fiber bundles, or whole muscle), *in situ* (muscle with intact vascularization and innervation but distal tendon attached to a force transducer), and *in vivo* (structures of the muscle or muscle unit remain intact). There are strengths and weaknesses to each of these preparations; however, a clear advantage of *in vivo* strength testing is the ability to perform repeated measurements in the same animal. Herein, the materials and methods to reliably assess isometric torque produced by the hindlimb dorsiflexor muscles *in vivo* in response to standard peroneal electrical stimulation in anesthetized pigs are presented.

Introduction

The primary function of skeletal muscle is to produce force, which ultimately makes activities such as breathing, eating, and ambulating possible. Conditions that reduce skeletal muscle functional capacity can lead to diminished performance (occupational or sport), disability, or death. For example, the maintenance of muscle mass and function in aging populations is positively associated with quality of life and the capacity to perform basic and instrumental

activities of daily living^{1,2}. And, declining muscle strength in Duchenne muscular dystrophy patients results in the inability to ambulate and respiratory failure, ultimately contributing to premature mortality^{3,4,5}. Thus, muscle strength measurement is a critical outcome measure in studies involving neuromuscular disease or injury.

Maximal voluntary isometric or isokinetic torque (and/or fatigue index) is often used as an index of

functional capacity in clinical studies⁶. In animal studies, analogous measurements can be made *in vivo* using electrical nerve stimulation while under anesthesia. Notably, *in vivo* preparations are minimally invasive with musculature, tendons, vasculature, and innervation remaining intact and therefore permit repeated functional assessments^{7,8,9,10,11}. This preparation is commonly used in small rodent models and to a lesser extent in larger animal models such as rabbits¹², dogs^{13,14}, sheep¹⁵, and pigs^{16,17}. The general use of such methodology could be impactful to many translational research studies, such as in genetically engineered porcine (pig) models of spinal muscular atrophy (SMA)¹⁸. Herein, methods to assess nerve stimulation-induced maximal isometric torque of the porcine dorsiflexor muscle group *in vivo* are presented. The techniques presented were initially adapted from those developed originally to assess mouse anterior crural muscle torque^{19,20} and subsequently refined through experience investigating torque producing capacity following injury^{17,21,22,23,24,25,26,27,28} and during development¹⁶ in various porcine models.

This protocol highlights *in vivo* isometric torque measurement using methodology that requires a computer integrated with a load cell and electrical stimulator. The methods presented here use a commercially available integrated Swine Isometric Footplate Test Apparatus, platform apparatus, and corresponding software (see **Table of Materials**). However, the methodology can be adapted to use other commercially available or custom-made software, data-acquisition devices, and stimulators. These methods are intended for use in a dedicated large animal surgical suite replete with standard equipment such as: locking surgical table, second locking table of equal height for the testing platform, ventilator and

monitoring devices, and heating mat or other devices to maintain body temperature.

The following team members are needed to conduct these methods: one skilled anesthesia technician and two study personnel to perform the functional testing. These people will work together for the initial stabilization of the limb on the platform apparatus. Then, one of the two personnel will be responsible for the electrode placement/positioning and the other for the computer applications during the testing.

Protocol

All animal experiments were conducted in compliance with the Animal Welfare Act, the implementing Animal Welfare Regulations, and the principles of the Guide for the Care and Use of Laboratory Animals. Prior testing has demonstrated that these methods are reliable²⁶ and have no adverse effects on the health or limb function of the pig. Testing has been conducted as often as weekly without any adverse events²³. Additionally, testing pre- and post-surgical interventions during the same day can be performed without placing untoward stress on the animal or inducing neuromuscular dysfunction.

1. Computer set up

1. Ensure initial set and calibration of the apparatus and components are conducted under manufacture specifications (see **Table of Materials**). Calibration using a range of weights from 0.2-2.5 kg is suggested.

NOTE: Torque is measured by a 140 mm foot-pedal (0.14 m) attached to a linear torque sensor with a 50 Newton-meter (N·m) capacity. The instrument's gain is set to scale to 25 N·m capacity by default to better match the anticipated torque production. Calibration is performed

by applying a known mass (e.g., 1 kg) to the foot-pedal at a known distance (e.g., 100 mm from the axis of rotation) and calculating torque. For example, 1 kg equals 9.806 N applied at 0.1 m is 0.9806 N·m torque. A relationship can then be established between torque applied to the torque sensor and the corresponding voltage output by the torque sensor. The author's torque sensors have confirmed the linearity of this relationship from 0.2-20 kg applied to a particular 40 cm calibration plate. Due to the length of the standard pedal, a calibration range of 0.2-2.5 kg is recommended. This produces enough signal to calculate the scale factor by linear regression.

2. Turn on the computer, stimulator, transducer system, and the analog-digital interface about 30 min before testing to allow stabilization of heat-related material changes that can impact electrical properties. Select the appropriate and connected data acquisition (DAQ) device.
3. Set up experimental parameters in the software as needed; the software allows for a saved study template. Prepare to set up the experiment (i.e., study template) to create a new study using the **Create a New Study** workbook option.
NOTE: Experimental parameters can be pre-loaded before beginning the study, which will result in prompts to include additional specific experiment information such as sex, body mass, date of birth, the time point of testing, treatment group, or similar variables as needed. The study setup parameters can be saved and used across the experiment.
4. Select the study previously created at the beginning of each evaluation. Add a **New Animal** if this is the first test for the pig to be tested and follow the prompt for the variables input into the study.

5. Click on **Prepare Experiment** once ready to begin the study, which will be needed to optimize electrode placement. Deliver repeat twitches to the nerve while determining optimal placement once the electrodes are placed (see step 3.6.).
6. Click on **Configure Instant Stim** first, and then adjust the pulse frequency, pulse width, number of pulses, train frequency, and run time.
7. Then, click on **Instant Sim** to deliver repeat twitches. Alternatively, push the **Manual Trigger** button on the Stimulator unit to manually give one twitch.
8. Open the **Live Data Monitor** during the study protocol when ready to start the whole experiment to allow real-time investigation/visualization of the contractions. Click on **Run Experiment** when prepared to begin the experiment (following animal preparation, see step 2).

2. Anesthesia preparation and maintenance

1. Fast male or female pigs, 40-90 kg, overnight before anesthesia event, allow water *ad libitum*. Obtain and record the correct bodyweight of the pig on the day of the procedure.
2. Induce anesthesia with intramuscular injections of tiletamine/zolzepam (Telazol, 4-6 mg/kg), xylazine (1-3 mg/kg), and propofol (2.6 mg/kg). Initially maintain with 5% isoflurane *via* facemask.
3. Intubate the pig with an endotracheal tube and place it on an automatic ventilator. Maintain the pig on peak pressure at 20 cm H₂O, an initial tidal volume of 10 mL/kg, and respiration rates at 8-12 breaths/min.

4. Adjust the ventilator setting to maintain an end-tidal PCO₂ of 40 ± 5 mmHg. Maintain anesthesia with 1%-3% isoflurane in 30%-37% O₂.

5. Maintain the body temperature of the pig at 37 °C for the duration of the protocol. Insert ear vein and Foley catheters for fluid delivery and urine collection, as needed.

NOTE: Using surgical plane anesthesia will prevent secondary contractions during the testing, especially from the gluteal muscles.

6. Monitor the depth of the anesthesia *via* eye reflex and position, lack of jaw tone, heart rate (range 80-150 bpm), systolic blood pressure (range 120-70 mmHg), or a combination of all these signs.

7. Prepare both the right and left hindlimbs once the pig is fully anesthetized and stable by first cleaning the limbs with soap and water to remove any debris and then shave the hair from the skin. Pay close attention to the lateral knee area, which will be used for electrode placement later.

8. Transport the pig to a surgical table and securely place it in the supine position. Position the pig toward the foot of the table with the gluteal muscles at or slightly over the end of the table.

NOTE: This will allow the surgical table and table holding the testing apparatus to abut.

9. Extubate the pig after the test and allow them to recover. Standard pig food and water should be replaced once the pig is fully recovered and can ambulate freely within the cage.

NOTE: Post-procedure analgesia is unnecessary for the *in vivo* testing alone; however, carprofen and/or buprenorphine SR can be provided per veterinary recommendation. Consultation with a local veterinarian is encouraged. The anesthesia and medications listed here are for guidance only and are currently approved at the University of Minnesota. Maintenance of anesthesia with isoflurane was chosen based on its rapid onset and offset and its minimal impact on *in vivo* nerve stimulation evoked torque²⁹. Take care to have consistency in anesthesia parameters across studies. During the protocol, anesthesia assessment and recording is conducted at 15 min intervals; recording is undertaken based on local Institutional Animal Care and Use Committee (IACUC) and United States Department of Agriculture (USDA) guidelines and requirements.

3. Evaluation of *in vivo* isometric torque

1. Place the foot on the foot-plate of the force transducer. Use a flexible cohesive bandage to attach the foot to the foot-plate.

NOTE: An entire role per foot is necessary; ideally, the 4-inch x 5-yard role is adequate.

2. Hold the foot in position on the foot-plate with the ankle at the neutral (A) and secure the foot to the plate by wrapping the cohesive bandage around the foot and foot-plate in the style of a closed basket weave ankle taping (B).

NOTE: The two study personnel will be required to simultaneously perform the individual (A) and (B) tasks.

3. Position the ankle at a right angle once the foot is secured to the foot-plate, defined as 0° or neutral for reference of degrees of plantar or dorsiflexion.



Figure 1: Pictures from various vantage points show the pig attachment to the foot-plate and anatomical alignment onto the frame. Anatomical landmarks for the anterior compartment muscles, fibular head, knee, tibial plateau, and femur are noted. Note the placement of subdermal electrode pairs on the lateral side of the leg. [Please click here to view a larger version of this figure.](#)

4. Stabilize the knee and ankle at right angles.
5. First, position the limb clamping bars close to the needed locations. When ready, starting on the medial aspect of the limb, align the limb clamping bar at about the tibial plateau.
6. Then, align the lateral limb clamping bar at the distal head of the femur.
NOTE: Between the end of each limb, the clamping bar uses a folded 4 x 4 gauze pad to protect the skin adjacent to the bar.
7. Stabilize the bars tightly using the locking thumbscrews.
NOTE: The limb clamping bars will not be in line with each other but will align with the pig's anatomy.
8. Clean the skin around the fibular head by applying 70% alcohol *via* clean gauze in concentric circles starting at the center of intended electrode placement and moving outwards. Place the sterile percutaneous needle (50 mm, 26 G monopolar) and electromyography (EMG)-style electrodes (see **Table of Materials**) across the peroneal nerve. Implant electrodes subdermally, approximately 5-10 mm.
9. Optimize the electrode placement using increasing current amplitudes, as adjusted on the stimulator. Start at 100 mA and increase as needed.
NOTE: 300-500 mA is usually required for peak twitch torque.
10. Visualize the twitch torque magnitude on the live data view and over the pig's anterior compartment; the hooves may splay and move upward as well.
11. Ensure that the posterior compartment, or tibia nerve, is not activated during stimulation. Visually inspect and palpate posterior compartment contraction and downward movement of hooves during stimulation.

12. Inspect the plateau region of tetanic contraction from the live torque-time tracing in the following steps for lack of antagonist muscle recruitment (i.e., plantarflexion for this protocol).
13. Elicit maximal isometric tetanic torque using the following stimulation parameters: 100 Hz, 0.1 ms pulse width, over an 800 ms train¹⁷, once the electrode placement and stimulation amplitudes are optimized.

NOTE: These parameters can be used for various contractile evaluations.

4. Protocol for torque-joint angle analysis

1. Measure the maximal isometric tetanic torque across a range of ankle positions ranging from neutral to the near end ranges of plantarflexion, or 0-50° of plantarflexion.

NOTE: Using 10° increments will require six contractions, and the incremental change can be adjusted for specific experimental questions.

2. Start loosening both locking screws of the goniometer stage to move between joint angles. Ensure both locking screws are tightened before the next contraction.

NOTE: The goniometer is scribed with degree markings to allow for precise alignment. It is likely 0° of plantar flexion, which is offset by 180° on the goniometer. Take caution to ensure intended positioning.

3. Determine the time between the contractions experimentally; however, 2 min is sufficient to avoid fatigue.

NOTE: As the ankle joint angle is incrementally changed, the needle electrodes may shift. It may be necessary to confirm the placement of the electrodes with twitch contractions, as noted above (see step 3.8).

5. Protocol for torque-frequency analysis

1. Position the ankle at the desired joint angle. Take care, experimentally, to conduct testing at the same joint angle each time.

NOTE: Typically, torque-frequency analyses are performed at a single joint angle corresponding with peak isometric torque derived from the torque-joint angle analysis. Peak torque is produced at ~30-35° of plantarflexion.

2. Measure maximal isometric torque over a range of stimulation frequencies that induce unfused trains of twitches up to and beyond those that induce fully fused tetani.

NOTE: This can be achieved by stimulating at 10, 20, 40, 60, and 100 Hz (0.1 ms pulse width; 800 ms train) with 2 min between each contraction to avoid fatigue. Depending on exact experimental questions and specific pig models, frequencies may be adapted. The bioenergetic substrate most likely utilized during an 800 ms contraction to maintain intracellular ATP is phosphocreatine³⁰, and the resynthesis of phosphocreatine relies on the phosphocreatine shuttle³¹. Phosphocreatine recovery kinetics indicate a 90% or more remarkable recovery between 90-120 s after contraction ends³⁰. Therefore, the recommended rest intervals between contractions are 90-120 s. Although, this may be influenced by experimental designs, including muscle disease, injury, and/or aging.

6. Data analysis

1. Click on **Analyze Results** if still in the software to open the Analysis window. Alternatively, open the Analysis program directly.
2. Whether using an automated data platform or manual analysis, calculate the different variables in analyzing individual isometric waveforms.

NOTE: These variables include: maximal twitch torque, maximal tetanic torque, and contractile properties related to twitches and tetani, e.g., time-to-peak and half-relaxation. Many experimental variables can normalize force, for example, body weight, muscle volume determined from MRI (magnetic resonance imaging) or CT (computed tomography), or terminal muscle weight. Both absolute torque (N·m) and torque normalized to body mass (N·m/kg) are presented. The resting torque placed on the foot-plate will differ across experiments. A baseline correction for resting torque should be applied to ensure true maximal twitch and tetanic torques are recorded. Baseline torque at each joint angle is recorded and can indicate changes in passive torque.

Representative Results

Reliability and optimization of the *in vivo* testing parameters of the anterior compartment of the pig have previously been reported²⁶. Comparative data across rodents and pigs for torque-frequency has also been reported²⁷.

During the *in vivo* assessment, visualization of the torque waveform is needed in real-time to ensure appropriate anterior compartment activation. The waveforms should only reflect dorsiflexion. The waveforms should have a smooth, rounded appearance and an apparent tetanic plateau (**Figure 2A**). Inconsistencies or perturbations of the waveform

indicate various experimental limitations, such as inadequate stimulation, improper electrode placement, or inadequate depth of anesthesia (**Figure 2B**).

Figure 3A is a twitch torque-time tracing with an arrow indicating 50% max torque. Time-to-peak contraction should start at the initiation of the stimulator and end when maximal twitch torque is achieved (representative time bars are shown below the tracing). Half-relaxation for a twitch should start at the maximal twitch torque and end at 50% maximal twitch torque (representative time bars are shown below the tracing). **Figure 3B** is a tetanic torque-time tracing with an arrow indicating 50% max torque. Unlike twitches that are ideal in terms of a definitive and timely maximal torque, tetanic contractions have greater variability in the timing of maximal torque concerning when the stimulator starts and ends, requiring a more nuanced approach to contractile property analysis. Time-to-peak contraction should begin with the initiation of the stimulator and stop somewhere between 90%-100% of maximal torque. The time bars in **Figure 3B** show a cutoff of 95% maximal torque. This is helpful in cases such as the selected representative data because the maximal torque is not reached until late in the plateau phase. A complementary analysis to time-to-peak is the average rate of contraction. The dashed bars on the ascending limb of the torque-time tracing represent a range of 30%-70% maximal torque. The average rate of contraction should be started at the start of stimulation and capture the average rate change between 30%-70% maximal torque. These are recommended ranges, and individual research groups can determine the ideal range around 50% (e.g., $\pm 10\%$). The important part is to be consistent within and across studies. In contrast to the twitch, tetanic contraction half-relaxation should start at the end of stimulation instead of maximal torque for the same reason mentioned above with time-to-peak. The time bars

in **Figure 3B** represent the time between the end of the stimulation and reaching 50% relaxation. A complementary analysis to half-relaxation is the average rate of relaxation. The dashed bars on the descending limb of the torque-tracing represent the same 30%-70% maximal torque range as the ascending limb. The average relaxation rate should start at the end of stimulation and capture the average rate of change between 30%-70% maximal torque. Again, these are recommended ranges. One critical note: do not confuse the average rate of contraction/relaxation with the maximal rate of contraction/relaxation. The maximal rate represents the single most remarkable rate change between two adjacent data points and can be widely variable.

Several twitch and contractile properties can be analyzed to gain insight into fiber type and excitation-contraction coupling attributes of the skeletal muscles^{10,32}. Over-interpretation of the twitch and contractile properties are cautioned; they represent suggestions and rationale for further cellular-level interrogation and are not necessarily indicative. In general, rates of contractility can reflect sarcoplasmic reticulum calcium release and myosin heavy chain isoform enzymatic rate. In contrast, relaxation rates can reflect sarco(endo)plasmic reticulum calcium ATPase enzyme rate and isoform. These properties can be influenced by fatigue, muscle damage, exercise training, and numerous pathologies (e.g., disuse atrophy).

Figure 4 depicts representative values for torque-frequency and torque-joint angle relationships for uninjured limbs. These data are representative of a wide range of pig sizes.

A representative, experimental analysis of surface EMG was conducted during *in vivo* muscle analysis (**Figure 5**) to demonstrate experimental control of rate coding and total muscle activity. Adhesive EMG electrodes were placed at the mid-belly of the peroneus tertius. A ground electrode was placed on the knee to minimize stimulation artifact, and stimulation electrode needles were placed around the peroneal nerve proximal to the muscle location. Simultaneous torque and EMG recordings were made at stimulation frequencies of 20, 60, and 100 Hz. The number of stimulator pulses (red bars in **Figure 5**) reflects the quotient of stimulation duration and time between pulses. For example, a 20 Hz stimulation frequency means a pulse every 50 ms; therefore, 400 ms stimulation duration divided by 50 ms between pulses equals eight pulses delivered (**Figure 5A**). The stimulator pulses are delivered to the nerve axon *via* percutaneous needle electrode placement and produce a similar number of electrical muscle pulses (i.e., 20 Hz equals 8 EMG recordings), demonstrating the experimental control of action potential frequency of the muscle group of interest. The raw EMG recordings can be converted *via* root-mean-square analysis (EMG RMS) to visualize the total muscle activity with increasing stimulation frequency. The area under the curve (AUC) analysis is one way to quantify the EMG RMS to determine changes in whole muscle activity. Representative AUCs for each EMG RMS stimulation frequency is provided (**Figure 5A-C**).

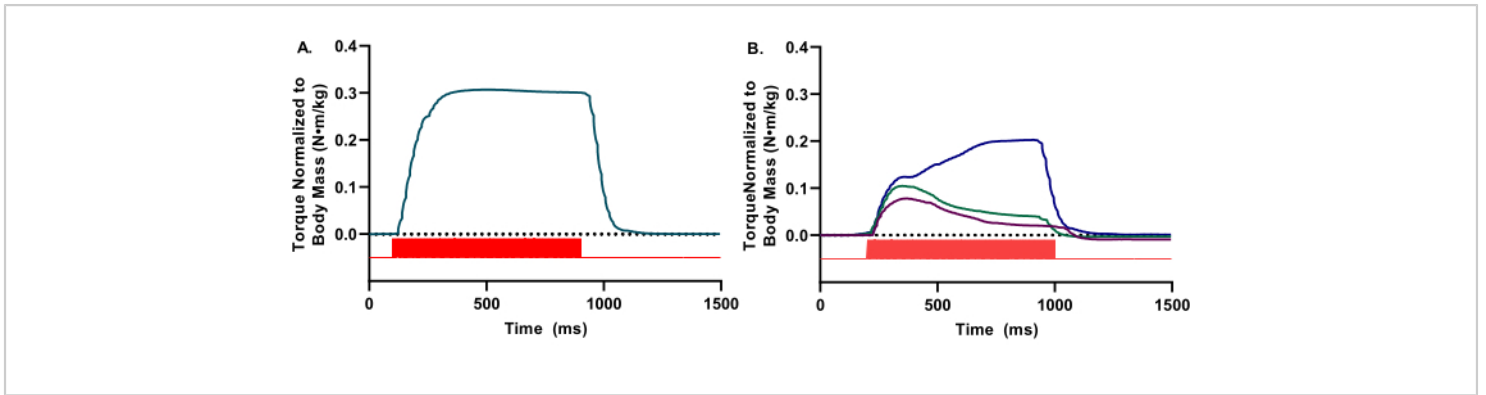


Figure 2: Representative high and low-quality waveforms. (A) Isometric waveforms present in a square-wave appearance, with a notable fluid plateau. (B) Low-quality waveforms can be due to inadequate stimulation or improper electrode placement. In these instances, repositioning of the electrodes is needed. For both A and B, the stimulator pulses (red bars) are indicated. [Please click here to view a larger version of this figure.](#)

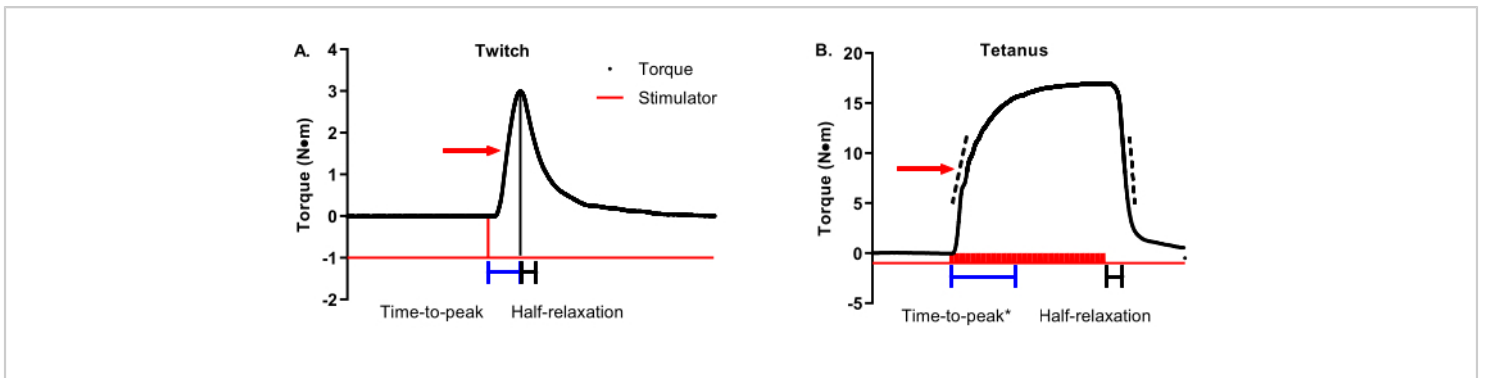


Figure 3: Twitch and tetanic contractile property analysis. (A) Representative twitch (1 Hz) and (B) tetanic (100 Hz) torque-time tracings are modified to detail contractile properties. The red arrow on each graph shows 50% maximal torque. Blue and black bars beneath the tracings show time-to-peak and half-relaxation time durations, respectively. Dashed bars on the ascending and descending limbs of the tetanic torque-time tracing represent a range of 30%-70% maximal torque that can be used to determine the average rate of contraction or relaxation. [Please click here to view a larger version of this figure.](#)

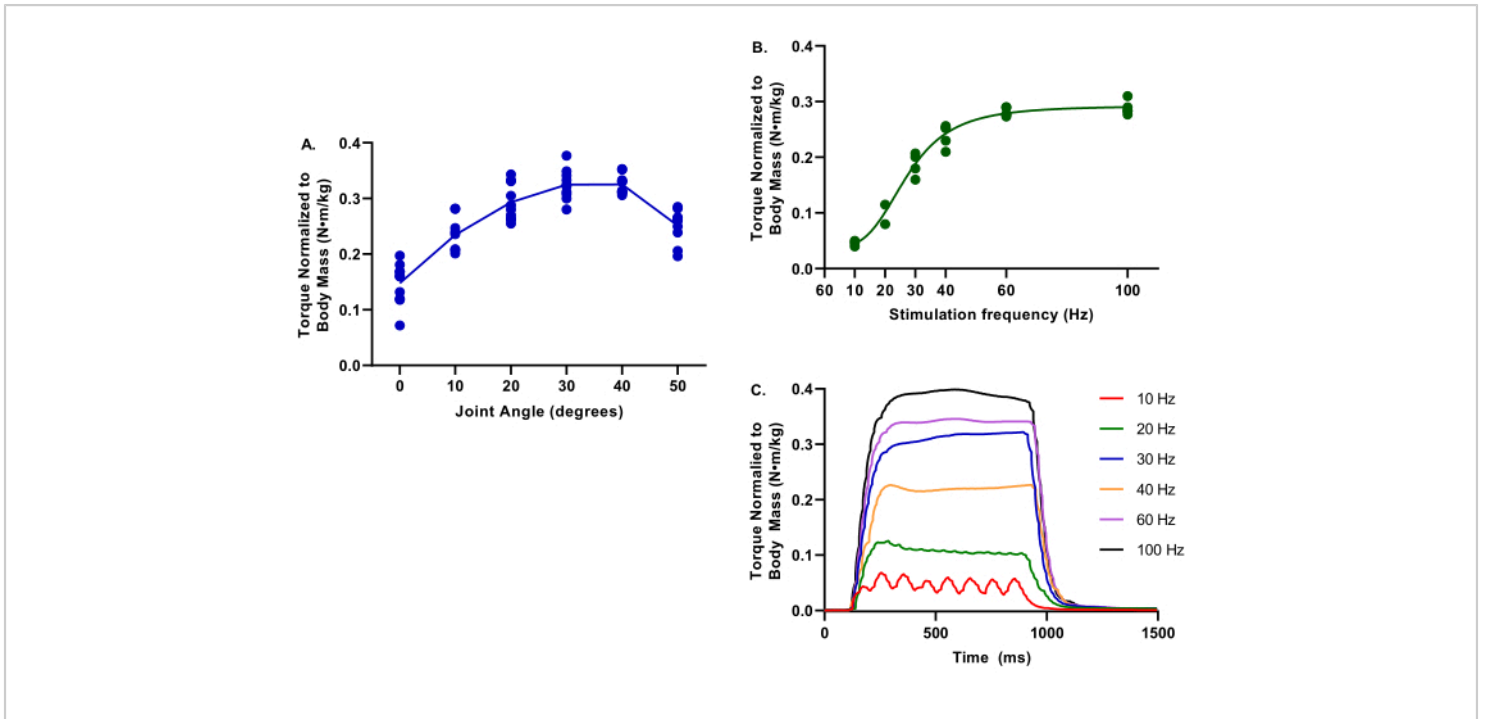


Figure 4: Example data of torque-joint angle and torque-frequency. Data provided is from a range of female Yorkshire Cross pigs at 2.9-6.3 months; 39.4-75.4 kg body mass; all considered healthy control at the evaluation time. During all testing, core body temperature was maintained at 37 °C. **(A)** Torque normalized to body mass is evaluated at ankle joints of 0-50° of plantarflexion; note the peak torque is determined at 30°. **(B)** Torque normalized to body mass is evaluated at various stimulation frequencies from 10-100 Hz; note these evaluations were conducted with the ankle joint at 30° of plantarflexion. **(C)** Individual torque tracings for each of the stimulation frequencies were evaluated. [Please click here to view a larger version of this figure.](#)

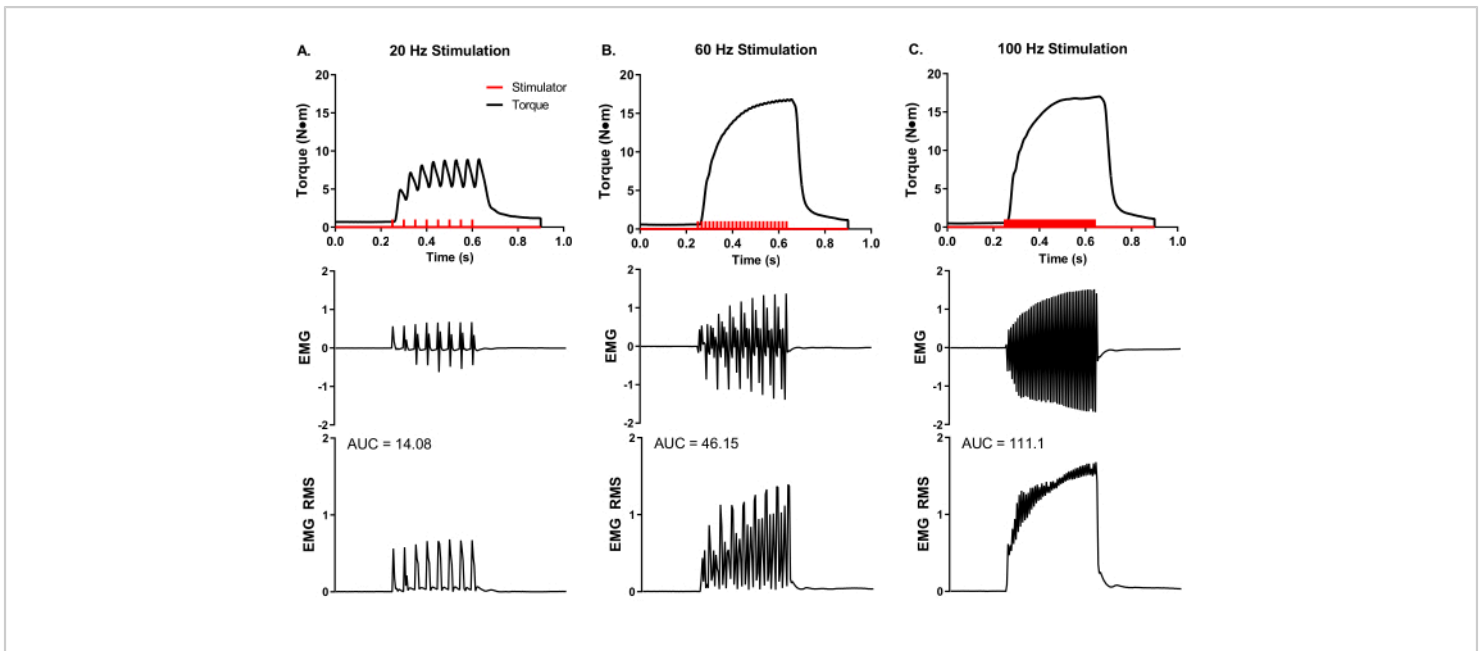


Figure 5: Concurrent *in vivo* isometric torque and EMG measurements. Simultaneous EMG and torque recordings at representative stimulation frequencies of (A) 20, (B) 60, and (C) 100 Hz collected from a female Yorkshire pig (~90 kg body mass). Stimulator pulses (red bars) were delivered according to the set stimulation frequency. Raw EMG recordings were converted to root-mean-square (EMG RMS) to visualize total muscle activity with increasing stimulation frequency. Representative EMG RMS curves were analyzed for the area under the curve (AUC), and AUCs are provided for each stimulation frequency. [Please click here to view a larger version of this figure.](#)

Discussion

Critical steps, modifications, and troubleshooting

For minimizing data variability and maximizing the approach's success, the following critical steps are highlighted.

Optimal nerve stimulation

This experimental approach starts with nerve axon depolarization and relies on correct electrode placement and optimized electrical stimulation. A post-mortem analysis of nerve anatomy related to boney landmarks can help visualize proper electrode placement during testing. Acquiring maximal twitch torque helps determine appropriate current (in milliamperes; mA) delivered to the nerve axon. There are two values to keep in mind when optimizing nerve stimulation

at the onset of testing: (1) the twitch-to-tetanic ratio is ~1:5, e.g., ~2 N·m twitch torque corresponds to a 10 N·m tetanic torque (Figure 3); and (2) the typical torque to body mass is ~0.3 N·m per kg body mass (Figure 4). If the peak twitch torques appear low, remove the electrodes and attempt another placement. Be sure to check stimulator settings, BNC connections, and electrode connections. Electrode re-placement may be needed in between contractions if there is too much movement during positioning of the limb between joint angles, as noted above (Figure 2). Please note experimental and interventional approaches could impact these values.

Proper biomechanical alignment

Starting muscle length influences muscle contractile force (the length-tension relationship), and muscle length can change based on hip, knee, and ankle joint alignment. The joint angles must be standardized between limbs and among pigs. A 90° ankle joint angle is strongly recommended for the hip and knee. A slightly plantarflexed ankle position (~30° from the neutral 0° ankle joint angle) is optimal for peak strength. It reflects the natural anatomical position of the ankle joint in both pigs and dogs while standing. All joints should also be parallel with the foot-pedal and torque transducers to avoid loss of measurable torque due to the contribution of a perpendicular torque vector. Inspecting the hip-knee-ankle joint angles and foot-pedal-joint alignment is strongly recommended after securing the foot to the foot-pedal and securing the knee joint with the limb clamping bars (**Figure 1**). If there is misalignment, unlock and remove the bars and reposition the pig on the surgical table. While standardizing joint angles across studies is critical for minimizing data variance, there are limitations to biomechanical alignment that are notable, discussed below.

Significance with respect to existing or alternative methods

Alternative examples of clinically relevant and non-invasive assessments of muscle function that could be used for porcine models include treadmill walking distance, EMG, and active muscle shear wave elastography. As the 6 min walk test in humans, a treadmill walking test can evaluate disease progression and intervention success in large animals^{33,34,35}. Typically, after an acclimation period, animals are walked until the end of compliance at different treadmill velocities and/or incline levels. Food rewards are often necessary to achieve maximal motivation. However, treadmill walking outcomes offer only indirect interpretations of muscle contractile function due to limitations such as

subject motivation, non-maximal motor unit recruitment, and inherent co-dependence on other body systems such as the cardiovascular, skeletal, and respiratory systems.

On the other hand, EMG offers a slightly better direct assessment of the skeletal muscle system, as EMG electrodes are placed directly on the muscle group of interest^{36,37,38}. EMG electrodes then measure the collective muscle activity (depolarized muscle fibers). This muscle activity is based on motor unit recruitment and rate coding (the frequency of action potentials sent to recruited motor units). However, separating the relative contributions of motor unit recruitment versus rate coding is impossible with surface EMG. Further, EMG relies on subject willingness to generate maximal contractions, and this level of cooperation is unlikely in large-animal models. While it can be informative to assess changes in EMG during the gait cycle, these data do not represent a maximal functional ability of the skeletal muscle group of interest. Ultrasound-based imaging utilizing B-mode and shear-wave elastography is another non-invasive modality used to evaluate muscle function. There is a good correlation between Young's modulus measured by elastography and increasing muscle loads^{39,40}. Shear-wave elastography has been validated and used as a quantitative measure of passive tissue stiffness^{41,42,43,44,45}, including in a porcine volumetric muscle loss injury model²³. It may also be used as an indirect measurement of active muscle force production³⁹. However, limitations akin to EMG for subject willingness and cooperation to perform contractions are still present.

The *in vivo* protocol described here, in contrast to treadmill walking distance and EMG, provides a reliable, reproducible, and maximal assessment of muscle function. This protocol evokes muscle contractions in a controlled, quantifiable

manner that is independent of motivation. Specifically, percutaneous electrodes are used to stimulate nerves axons bypassing the central nervous system. Depolarization of the nerve axons engages all motor units eliminating variability associated with motor unit recruitment. Additionally, the investigator controls rate coding (stimulation frequency). The resulting neuromuscular physiology that applies to this approach starts with voltage-gated sodium channel activation at the nodes of Ranvier. All subsequent (or downstream) physiology is engaged, including excitation-contraction coupling and cross-bridge cycling. A significant advantage of the *in vivo* non-invasive muscle analysis is that contractile muscle function can be measured repeatedly, for example, weekly, to monitor muscle strength after injury, intervention, or over a disease progression.

Limitations of the method

The *in vivo* equipment described in this protocol permits passive and active isometric torque as a function of joint angle and stimulation frequency. The testing apparatus used does not support the measurement of dynamic contractions (e.g., isokinetic eccentric or concentric contractions). The apparatus allows a 105° range of motion to characterize the torque-joint angle relationship and uses a load cell with a maximum torque range of ~50 N·m. Specific experimental questions may require performance characteristics outside of these specifications. Notably, the load cell on this described apparatus may be exchanged for greater torque ranges if needed.

The protocol described herein to measure maximal neuromuscular strength *in vivo* has notable limitations. First, this method requires anesthesia, which may be conducted differently per animal facility protocols and resources. Anesthetics are known to have varying effects on

neuromuscular function and have been shown to alter mouse *in vivo* dorsiflexor torque production in an anesthetic-type and -dose-dependent manner²⁹. The differential effects of anesthetics on the large-animal *in vivo* torque are unclear; therefore, control and experimental groups must have the same anesthesia agents (e.g., all groups administered ketamine) to control this variability. Second, reliance on *in vivo* diffusion patterns limits exploration of cellular mechanisms of contractile dysfunction and acute drug toxicities. For example, caffeine can be used during *in vitro* organ bath testing of an isolated muscle to stimulate sarcoplasmic reticulum calcium release, bypassing excitation-contraction coupling⁴⁶ directly. The amount of caffeine to induce this effect (mM) is lethal in an *in vivo* setting. Drug influences on the whole body (e.g., kidney/liver stress) and subsequent factors secreted into circulation will need to be considered if this approach is used for drug screening on acute muscle strength²³. Third, the use of maximal electrical nerve stimulation deviates from voluntary recruitment strategies, as discussed above, and therefore does not reflect changes in strength that may be due to neuromuscular recruitment adaptations.

In vivo torque measurements may also be limited with regard to establishing a specific mechanism for experimental observations. For instance, torque about the ankle joint depends not only on muscle force production but also on the tendon and joint and connective tissue properties. Moreover, force is generated by groups of muscles, specifically the plantar flexors (gastrocnemius, soleus, and plantaris muscles) and the dorsiflexors (peroneus tertius, tibialis, and digitorum muscles) in pigs. Therefore, interpretations of maximal *in vivo* torque data require consideration of potential musculotendinous and anatomical changes and are limited to muscle groups, not individual muscles. Relatedly, muscle groups are often made up of a mixture of predominately

fast- and slow-muscle fibers, such as the gastrocnemius and soleus muscle, respectively, of the plantar flexors. Contractile properties such as rate of contraction and relaxation (or time-to-peak contraction and half-relaxation time) are not reliable indicators of fiber type physiology using *in vivo* versus isolated muscle preparations, such as *in vitro* or *in situ* testing protocols⁴⁷. Isolated muscle preparations are also superior in understanding the influence of biomechanical parameters on muscle function because properties such as muscle length can be precisely controlled; it is important to stress that the joint angle-torque relationship is not directly equivalent to the muscle length-force relationship, as tendon (e.g., slack), muscle (e.g., pennation angle, sarcomere overlap), and joint (e.g., moment arm) properties that contribute to torque production are dependent on the joint angle. To that end, large animal *in situ* functional testing⁴⁸ could be a valuable addition to *in vivo* testing, bearing in mind that *in situ* testing is a terminal experiment. Other advancements to the current protocol that may be explored in the future to improve the mechanistic insight of experimental findings include using ultrasound B-mode imaging to measure muscle and tendon architectural properties and implantation of a tendon force transducer to measure muscle force during voluntary and electrically stimulated contractions⁴⁹.

Importance and potential applications of the method

This protocol evaluates *in vivo* torque-producing capacity of the porcine dorsiflexor muscle group, demonstrating a non-invasive method to assess gain or loss of muscle function in a physiological setting. Because the methodology is non-terminal to the pig, it can also be used to evaluate muscle function in the same subjects longitudinally during the progression of a disease, or before, during, and following a treatment strategy. As such, a repeated measures experimental design may allow for robust

statistical comparisons with greater power and fewer animals compared to independent measures. Additionally, skeletal muscle dysfunction is a salient component of various disease processes and conditions, such as chronic disease-associated muscle wasting (e.g., heart failure, kidney failure, AIDS, cancer, etc.), muscular dystrophy, neurodegenerative diseases (e.g., SMA or amyotrophic lateral sclerosis; ALS), aging (i.e., sarcopenia), and drug toxicities. Skeletal muscle functional capacity is a critical primary outcome measure for interventions such as exercise, nutrition, and drug and regenerative medicine therapies. Thus, the protocol described herein to reliably evaluate porcine torque producing capacity *in vivo* may be used across numerous study applications. It may be instrumental in acquiring extensive animal data for the translation of developing therapies.

Disclosures

The opinions or assertions contained here are the private views of the authors. They are not to be construed as official or as reflecting the views of the Department of the Army, the Department of Defense, or the United States Government.

The production of the video article and Open Access availability was sponsored by Aurora Scientific, Inc. Matthew Borkowski is employed by Aurora Scientific Inc. This company may potentially benefit from the research results.

Acknowledgments

Work and data presented were supported broadly by the US Army Medical Research and Materiel Command to BTC and SMG (#MR140099; #C_003_2015_USAISR; #C_001_2018_USAISR); and the Department of Veterans Affairs, Veterans Health Administration, Office of Research and Development (I21 RX003188) to JAC and Dr. Luke Brewster. The authors gratefully acknowledge the USAISR

Veterinary Service and Comparative Pathology Branches and UMN Advanced Preclinical Imaging Center for technical assistance in completing these studies.

References

1. Verlaan, S. et al. Nutritional status, body composition, and quality of life in community-dwelling sarcopenic and non-sarcopenic older adults: A case-control study. *Clinical Nutrition*. **36** (1), 267-274 (2017).
2. Wang, D. X. M., Yao, J., Zirek, Y., Reijnierse, E. M., Maier, A. B. Muscle mass, strength, and physical performance predicting activities of daily living: a meta-analysis. *Journal of Cachexia, Sarcopenia and Muscle*. **11** (1), 3-25 (2020).
3. Ishikawa, Y. et al. Duchenne muscular dystrophy: survival by cardio-respiratory interventions. *Neuromuscular Disorders*. **21** (1), 47-51 (2011).
4. Khirani, S. et al. Respiratory muscle decline in Duchenne muscular dystrophy. *Pediatric Pulmonology*. **49** (5), 473-481 (2014).
5. Ziter, F. A., Allsop, K. G., Tyler, F. H. Assessment of muscle strength in Duchenne muscular dystrophy. *Neurology*. **27** (10), 981-984 (1977).
6. Garg, K. et al. Volumetric muscle loss: persistent functional deficits beyond frank loss of tissue. *Journal of Orthopaedic Research*. **33** (1), 40-46 (2015).
7. Lovering, R. M., Roche, J. A., Goodall, M. H., Clark, B. B., McMillan, A. An in vivo rodent model of contraction-induced injury and non-invasive monitoring of recovery. *Journal of Visualized Experiments: JoVE*. (51), e2782 (2011).
8. Mintz, E. L., Passipieri, J. A., Lovell, D. Y., Christ, G. J. Applications of in vivo functional testing of the rat tibialis anterior for evaluating tissue engineered skeletal muscle repair. *Journal of Visualized Experiments: JoVE*. (116), e54487 (2016).
9. Call, J. A., Warren, G. L., Verma, M., Lowe, D. A. Acute failure of action potential conduction in mdx muscle reveals new mechanism of contraction-induced force loss. *The Journal of Physiology*. **591** (Pt 15), 3765-3776 (2013).
10. Call, J. A., Eckhoff, M. D., Baltgalvis, K. A., Warren, G. L., Lowe, D. A. Adaptive strength gains in dystrophic muscle exposed to repeated bouts of eccentric contraction. *The Journal of Physiology*. (1985). **111** (6), 1768-1777 (2011).
11. Ingalls, C. P., Wenke, J. C., Nofal, T., Armstrong, R. B. Adaptation to lengthening contraction-induced injury in mouse muscle. *The Journal of Physiology*. (1985). **97** (3), 1067-1076 (2004).
12. Hyman, S. A. et al. In vivo supraspinatus muscle contractility and architecture in rabbit. *The Journal of Physiology*. (1985). **129** (6), 1405-1412 (2020).
13. Childers, M. K., Grange, R. W., Kornegay, J. N. In vivo canine muscle function assay. *Journal of Visualized Experiments: JoVE*. (50), e2623 (2011).
14. Grange, R. W. et al. Muscle function in a canine model of X-linked myotubular myopathy. *Muscle & Nerve*. **46** (4), 588-591 (2012).
15. Novakova, S. S. et al. Repairing volumetric muscle loss in the ovine peroneus tertius following a 3-month recovery. *Tissue Engineering Part A*. (2020).

16. Maeng, G. et al. Humanized skeletal muscle in MYF5/MYOD/MYF6-null pig embryos. *Nature Biomedical Engineering*. (2021).
17. Ward, C. L. et al. Autologous minced muscle grafts improve muscle strength in a porcine model of volumetric muscle loss injury. *Journal of Orthopaedic Trauma*. **30** (12) e396-e402 (2016).
18. Prather, R. S., Lorson, M., Ross, J. W., Whyte, J. J., Walters, E. Genetically engineered pig models for human diseases. *Annual Review of Animal Biosciences*. **1**, 203-219 (2013).
19. Lowe, D. A., Warren, G. L., Ingalls, C. P., Boorstein, D. B., Armstrong, R. B. Muscle function and protein metabolism after initiation of eccentric contraction-induced injury. *Journal of Applied Physiology* (1985). **79** (4), 1260-1270 (1995).
20. Ashton-Miller, J. A., He, Y., Kadhiresan, V. A., McCubbrey, D. A., Faulkner, J. A. An apparatus to measure in vivo biomechanical behavior of dorsi- and plantarflexors of mouse ankle. *Journal of Applied Physiology* (1985). **72** (3), 1205-1211 (1992).
21. Chao, T., Burmeister, D. M., Corona, B. T., Greising, S. M. Oxidative pathophysiology following volumetric muscle loss injury in a porcine model. *Journal of Applied Physiology* (1985). **126** (6), 1541-1549 (2019).
22. Corona, B. T., Greising, S. M. Challenges to acellular biological scaffold mediated skeletal muscle tissue regeneration. *Biomaterials*. **104**, 238-246 (2016).
23. Corona, B. T., Rivera, J. C., Dalske, K. A., Wenke, J. C., Greising, S. M. Pharmacological Mitigation of Fibrosis in a Porcine Model of Volumetric Muscle Loss Injury. *Tissue Engineering Part A*. (2020).
24. Corona, B. T., Rivera, J. C., Greising, S. M. Inflammatory and physiological consequences of debridement of fibrous tissue after volumetric muscle loss injury. *Clinical and Translational Science*. **11** (2), 208-217 (2018).
25. Corona, B. T., Rivera, J. C., Wenke, J. C., Greising, S. M. Tacrolimus as an adjunct to autologous minced muscle grafts for the repair of a volumetric muscle loss injury. *Journal of Experimental Orthopaedics*. **4** (1), 36 (2017).
26. Greising, S. M. et al. Unwavering pathobiology of volumetric muscle loss injury. *Scientific Reports*. **7** (1), 13179 (2017).
27. Pollot, B. E., Corona, B. T. Volumetric muscle loss. *Methods in Molecular Biology*. **1460**, 19-31 (2016).
28. Kheirabadi, B. S. et al. Long-term effects of Combat Ready Clamp application to control junctional hemorrhage in swine. *The Journal of Trauma and Acute Care Surgery*. **77** (3 Suppl 2), S101-108 (2014).
29. Ingalls, C. P., Warren, G. L., Lowe, D. A., Boorstein, D. B., Armstrong, R. B. Differential effects of anesthetics on in vivo skeletal muscle contractile function in the mouse. *Journal of Applied Physiology*. **80** (1), 332-340 (1996).
30. Forbes, S. C., Paganini, A. T., Slade, J. M., Towse, T. F., Meyer, R. A. Phosphocreatine recovery kinetics following low- and high-intensity exercise in human triceps surae and rat posterior hindlimb muscles. *American Journal of Physiology. Regulatory, Integrative and Comparative Physiology*. **296** (1), R161-170 (2009).
31. Meyer, R. A., Sweeney, H. L., Kushmerick, M. J. A simple analysis of the "phosphocreatine shuttle." *American Journal of Physiology*. **246** (5 Pt 1), C365-377 (1984).

32. McKeehen, J. N. et al. Adaptations of mouse skeletal muscle to low-intensity vibration training. *Medicine & Science in Sports & Exercise*. **45** (6), 1051-1059 (2013).
33. Boakye, M. et al. Treadmill-based gait kinematics in the yucatan mini pig. *Journal of Neurotrauma*. **37** (21), 2277-2291 (2020).
34. Woodman, C. R., Muller, J. M., Laughlin, M. H., Price, E. M. Induction of nitric oxide synthase mRNA in coronary resistance arteries isolated from exercise-trained pigs. *American Journal of Physiology*. **273** (6), H2575-2579 (1997).
35. Boddy, K. N., Roche, B. M., Schwartz, D. S., Nakayama, T., Hamlin, R. L. Evaluation of the six-minute walk test in dogs. *American Journal of Veterinary Research*. **65** (3), 311-313 (2004).
36. Valentin, S., Zsoldos, R. R. Surface electromyography in animal biomechanics: A systematic review. *Journal of Electromyography & Kinesiology*. **28**, 167-183 (2016).
37. Stegeman, D. F., Blok, J. H., Hermens, H. J., Roeleveld, K. Surface EMG models: properties and applications. *Journal of Electromyography & Kinesiology*. **10** (5), 313-326 (2000).
38. Zwarts, M. J., Stegeman, D. F. Multichannel surface EMG: basic aspects and clinical utility. *Muscle Nerve*. **28** (1), 1-17 (2003).
39. Liu, J. et al. Non-invasive quantitative assessment of muscle force based on ultrasonic shear wave elastography. *Ultrasound in Medicine and Biology*. **45** (2), 440-451 (2019).
40. Wang, A. B., Perreault, E. J., Royston, T. J., Lee, S. S. M. Changes in shear wave propagation within skeletal muscle during active and passive force generation. *Journal of Applied Biomechanics*. **94**, 115-122 (2019).
41. Brandenburg, J. E. et al. Quantifying passive muscle stiffness in children with and without cerebral palsy using ultrasound shear wave elastography. *Developmental Medicine & Child Neurology*. **58** (12), 1288-1294 (2016).
42. Brandenburg, J. E. et al. Ultrasound elastography: the new frontier in direct measurement of muscle stiffness. *Archives of Physical Medicine and Rehabilitation*. **95** (11), 2207-2219 (2014).
43. Brandenburg, J. E. et al. Feasibility and reliability of quantifying passive muscle stiffness in young children by using shear wave ultrasound elastography. *Journal of Ultrasound in Medicine*. **34** (4), 663-670 (2015).
44. Eby, S. F. et al. Shear wave elastography of passive skeletal muscle stiffness: influences of sex and age throughout adulthood. *Clinical Biomechanics (Bristol, Avon)*. **30** (1), 22-27 (2015).
45. Eby, S. F. et al. Validation of shear wave elastography in skeletal muscle. *Journal of Biomechanics*. **46** (14), 2381-2387 (2013).
46. Ingalls, C. P., Warren, G. L., Williams, J. H., Ward, C. W., Armstrong, R. B. E-C coupling failure in mouse EDL muscle after in vivo eccentric contractions. *Journal of Applied Physiology (1985)*. **85** (1), 58-67 (1998).
47. Warren, G. L., Lowe, D. A., Armstrong, R. B. Measurement tools used in the study of eccentric contraction-induced injury. *Sports Medicine*. **27** (1), 43-59 (1999).
48. Dobson, J. L., Gladden, L. B. Effect of rhythmic tetanic skeletal muscle contractions on peak muscle perfusion.

Journal of Applied Physiology (1985). **94** (1), 11-19 (2003).

49. Fleming, B. C., Beynnon, B. D. In vivo measurement of ligament/tendon strains and forces: a review. *Annals of Biomedical Engineering*. **32** (3), 318-328 (2004).